Formation of Hydroxyl Radical from the Hydrogen Chemisorbed Silicon Surface by Incident Oxygen Atoms

Jongbaik Ree,* **Kyung Soon Chang, Yoo Hang Kim,[†] and Hyung Kyu Shin[‡]**

Department of Chemistry Education, Chonnam National University, Gwangju 500-757, Korea
[†]*Department of Chemistry and Center for Chemical Dynamics, Inha University, Inchon 402-751, Korea*
[‡]*Department of Chemistry, University of Nevada, Reno, Nevada 89557, U.S.A.*
Received April 16, 2003

We have calculated the probability of the OH formation and energy deposit of the reaction exothermicity in the newly formed OH, particularly in its vibrational motion, in the gas-surface reaction $O(g) + H(ad)/Si \rightarrow OH(g) + Si$ on the basis of the collision-induced Eley-Rideal mechanism. The reaction probability of the OH formation increases linearly with initial excitation of the HSi vibration. The translational and vibrational motions share most of the energy when the H-Si vibration is initially in the ground state. But, when the initial excitation increases, the vibrational energy of OH rises accordingly, while the energies shared by other motions vary only slightly. The product vibrational excitation is significant and the population distribution is inverted. Flow of energy between the reaction zone and the solid has been incorporated in trajectory calculations. The amount of energy propagated into the solid is only a few percent of the available energy released in the OH formation.

Key Words : Hydroxyl, Hydrogen, Silicon, Oxygen, Eley-Rideal

Introduction

In gas-adatom interactions taking place on a solid surface, important reactive events involve the dissociation of the adatom-surface bond and association of the gas atom with the desorbing adatom. Such reactions are often highly exothermic, so there is a large amount of energy to be deposited in the various motions of the product. For example, chemisorption energies of atoms such as hydrogen and oxygen on a close-packed metal surface lie in the range of 2-3 eV,[1,2] whereas the energy of the bond formed between such atoms is 4-5 eV.[3] Thus, the reaction exothermicity is about 2 eV, which is to be distributed among various motions of the product, including the solid phase. An Eley-Rideal (ER) mechanism has been proposed to study such exothermic gas-surface reactions, most involving chemisorbed hydrogen atoms.[4-10] The exothermicity is still very significant in the reactions involving a nonmetallic surface such as graphite or silicon.[11-18] In such reactions where the surface is covered either sparsely or completely by chemisorbed hydrogen atoms, the possible reaction pathways involve the production of H_2 or other H-containing molecules. The characterization of time evolution of such reactive events and energy disposal in the product is important in elucidating the mechanistic details. Furthermore, such reactions can produce active surface sites, which can subsequently react with incident or pre-adsorbed molecules or atoms. While the reactions taking place on a metallic surface are important on studying catalysis, those occurring on a silicon surface are of importance in the processing of silicon-based materials.

In the present paper, we study the oxygen atom abstraction of hydrogen chemisorbed on a silicon surface, $O(g) + H(ad)/Si \rightarrow OH(g) + Si$ with particular emphasis on the disposal of the reaction exothermicity in the vibrational motion of OH varying the initial excitation of the adatom-surface vibration from $v_{HSi} = 0$ to 3. We will use a modified version of the London-Eyring-Polanyi-Sato (LEPS) procedure, which includes additional energy terms that result from the participation of adjacent surface sites in the oxygen-to-surface interaction,[19] for the potential energy surface and use it in the molecular time scale generalized Langevin equation (MTGLE), which is designed to describe the combined motions of reaction-zone atoms and surface atoms.[20,21] The incorporation of surface atom dynamics enables us to determine the flow of energy between the reaction zone and the solid in an accurate way. We consider the reaction that takes place at a gas temperature of 1500 K and surface temperature of 300 K.

Model

The interaction model and numerical procedures have already been reported in Ref. 19. We briefly summarize the essential aspect of the model for the interaction of atomic oxygen with H chemisorbed on the Si(001)−(2 × 1) surface reconstructed by dimer formation along the [110] direction. For easy reference we display the collision model in Figure 1 defining the pertinent coordinates. The H atom is chemisorbed on the Si atom of the symmetric dimer structure. This adatom site, which is surrounded by eight adjacent Si atom, is the $N = 0$ member of the $(N + 1)$-atom chain, which links the reaction zone to the heat bath. We shall refer to this adatom site as the zeroth Si atom. Thus, in addition to the adatom, the incident atom is in interaction with all these $8 + (N + 1)$ Si atoms, where the zeroth atom on which the hydrogen atom is

Hydroxyl Radical from the Hydrogen on Silicon

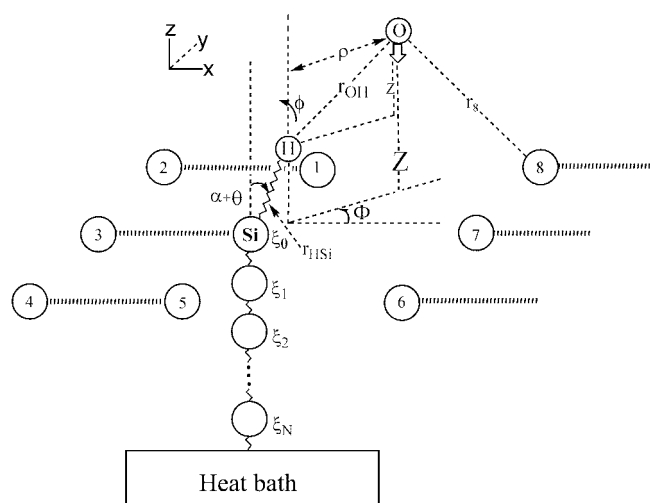*Bull. Korean Chem. Soc.* **2003**, Vol. 24, No. 7   987

Figure 1. Interaction model. The zeroth atom on which H is adsorbed is surrounded by eight adjacent Si atoms. The *N*-atom chain connects the HSi vibration to the heat bath. The coordinates (r_{HSi}, θ, ϕ) for H, (ρ, Z, Φ) for O, and ξ's for the *N* chain atoms are defined. α is the tilt angle, r_{OH} is the O to H distance, and r_i is the O to the *i*th surface-layer Si distance (only r_8 is indicated).

chemisorbed, is surrounded by eight surface-layer Si atoms and the last (*N*th) atom is bound to the bulk phase. All these interaction energy terms are included in a modified version of the LEPS potential energy surface. Since the gas atom-to-nine surface atom distances have the functional dependence $r_i \equiv r_i(r_{HSi}, \theta, \phi, \rho, Z, \Phi)$ and the O(g)-to-H(ad) distance $r_{OH} \equiv r_{OH}(r_{HSi}, \theta, \rho, Z)$, we can obtain the potential energy $U(r_{HSi}, \theta, \phi, \rho, Z, \Phi, \{\xi\})$, where $\{\xi\}$ is the collective notation for $(\xi_0, \xi_1, ..., \xi_N)$ describing the vibrational coordinates of the $(N+1)$-chain atoms. Here, we have transformed the coordinate of the incident gas atom (x_O, y_O, z_O) into the cylindrical system (ρ, Z, Φ) and the adatom coordinate (x_H, y_H, z_H) into (r_{HSi}, θ, ϕ). The adatom is tilted by $\alpha = 20.6°$.[22]

Each Coulomb or exchange term of the LEPS potential function contains the Sato parameter (Δ). By varying their values systematically, we find the Sato parameters which best describe the desired features of minimizing barrier height and attractive well depth in both the entrance and exit channels to be $\Delta_{OH} = 0.50$, $\Delta_{HSi} = 0.05$, $\Delta_{OS} = 0.20$ for the oxygen-to-eight surface-layer Si atom interactions, and $\Delta_{OS} = 0.50$ for the oxygen-to-zeroth Si atom. The attractive potential energy surface constructed with these parameters is shown in Figure 2, where both the fine and coarse plots are presented. In Figure 2(b), we find the barrier height of 0.78 kcal/mol for O(g) + H(ad)/Si. In a related system of H(g) + H(ad)/Si, the observed activation energies of D(g) + H(ad)/Si and H(g) + D(ad)/Si are 1.06 ± 0.11 kcal/mol and 0.55 ± 0.05 kcal/mol,[11] respectively. A positive value of Δ tends to favor formation of the indicated bond and a negative value tends to promote the dissociation. Although the above set eliminates an attractive potential well in the product channel, it produces a very shallow well of the depth of about 0.25 kcal/mol in the entrance channel.

To study the reactive event, we follow the time evolution

of the reaction system by integrating the equations of motion, which describe the motions of the reaction-zone atoms and *N*-chain atoms. An intuitive way to treat the dynamics of the reaction involving many surface atoms is to solve the motions of primary zone atoms governed by the MTGLE set of the equations for the gas atom, adatom, zeroth Si atom and *N* chain atoms. The equations of motion for the gas atom and adatom are in the form

$$m_j \ddot{Y}_j(t) = -\partial U(r_{HSi}, \theta, \phi, \rho, Z, \Phi, \{\xi\})/\partial Y_j \qquad (1)$$

where $j = 1, 2, ..., 6$ for $Z, \rho, \Phi, r_{HSi}, \theta, \phi$, with $m_1 = m_O$, $m_2 = \mu_{OH}$, $m_3 = I_{OH}$, $m_4 = \mu_{HSi}$, and $m_5 = m_6 = I_{HSi}$. Here μ is the reduced mass and I is the moment of inertia. The potential energy contains the effects of all surface-layer atoms. For the $(N + 1)$-atom chain dynamics, we have[19]

$$\ddot{\xi}_0 = -\omega_{e0}^2 \xi_0(t) + \omega_{c1}^2 \xi_1(t)$$
$$- M_s^{-1} \partial U(r_{HSi}, \theta, \phi, \rho, Z, \Phi, \{\xi\})/\partial \xi_0, \qquad (2a)$$

$$\ddot{\xi}_1 = -\omega_{e1}^2 \xi_1(t) + \omega_{c1}^2 \xi_0(t) + \omega_{c2}^2 \xi_2(t), \qquad (2b)$$

$$\ddot{\xi}_j = -\omega_{e,j}^2 \xi_j(t) + \omega_{c,j}^2 \xi_{j-1}(t) + \omega_{c,j+1}^2 \xi_{j+1}(t),$$
$$j = 2, 3, ..., N-1 \qquad (2c)$$

$$\ddot{\xi}_N(t) = -\Omega_N^2 \xi_N(t) + \omega_{c,N}^2 \xi_{N-1}(t) - \beta_{N+1} \dot{\xi}_N(t) + f_{N+1}(t). \qquad (2d)$$

In these equations, M_s is the mass of the silicon atom, ω_e the Einstein frequency, ω_c the coupling frequency characterizing the chain, and Ω_N the adiabatic frequency. The quantity $f_{N+1}(t)$ determines the random force on the primary system arising from thermal fluctuation in the heat bath. The friction coefficient β_{N+1} is very close to $\pi \omega_D/6$, where ω_D is the Debye frequency.[20] The Debye temperature of Si is 640 K.[23] All values of the frequencies and friction coefficients are presented elsewhere.[24] The initial conditions needed to solve these equations have already been given in earlier papers.[14]

The numerical procedures include an extensive use of Monte Carlo routines to generate random numbers for initial conditions. The first step is to sample collision energies E from a Maxwell distribution at the gas temperature T_g and to weigh the initial energy of H(ad)-Si$_0$ and all chain atom vibrations by a Boltzmann distribution at the surface temperature T_s. The normal component of the incident energy is $E\cos^2\theta_{inc}$, which will be used in solving the equations of motion, where $\theta_{inc} = \tan^{-1}(\rho/z)$ and $z = Z - r_{HSi}\cos(\alpha + \theta)$. In sampling impact parameters, we take the flat range of $0 \leq b \leq b_{max}$, where $b_{max} = (3.057 + 1/2 \times 5.153)$ Å $= 5.633$ Å. Here 3.057 Å is the horizontal distance between the equilibrium position of H(ad) and the surface normal axis through the third Si (2.524 Å + 1.514 Å $\sin\alpha$), and 5.153 Å is the nearest Si-Si distance between two different strands (*i.e.*, zeroth and seventh Si).[22] This wide range of b will enable us to treat all trajectories, including those approaching the third Si from the left-hand side which is important in the reaction. Also sampled are the initial values
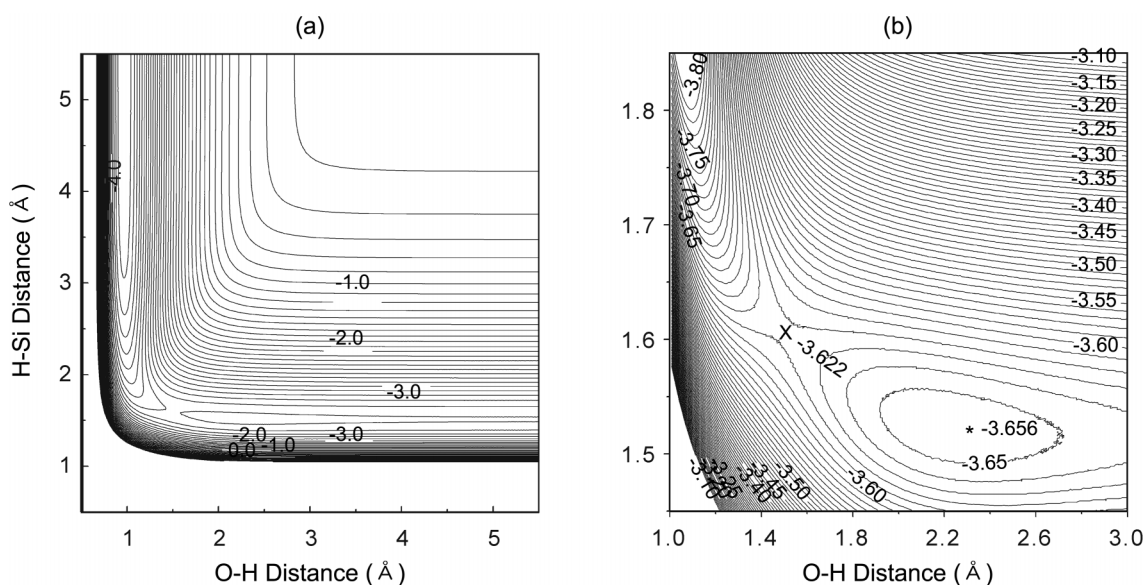
Figure 2. Attractive potential energy surface in (a) coarse scale and (b) fine scale in the direction of $\theta = \phi = \Phi = 0°$ for the $b = 0$ collision. In (b) the position of the barrier is indicated by "×" at −3.622 eV. The star indicates the position of the potential minimum (−3.656 eV) in the entrance channel. The labeled contours are in electron volts; they are in (a) 0.25 eV interval and (b) 0.010 eV interval.

Table 1. Interaction Parameters for O(g) + H(ad)/Si

Interaction (i)	OH	H-Si	O-surface
$D_{0,i}^{0}$ (eV)[a]	4.392	3.50	3.82
ω_i (cm^{-1})[b]	3738	2093	972
d_i (Å)[c]	0.9697	1.514	1.709
a_i (Å)[d]	0.2178	0.334	0.185

[a]$D_i = D_{0,i}^{0} + 1/2\hbar\omega_i$ (ref. 25 for OH; refs. 26 and 27 for H-Si; ref. 28 for O-Si). [b]Ref. 25 for O-H; refs. 12 and 29 for H-Si; ref. 28 for O-Si. Here the H-Si value 2093 cm^{-1} is the z-direction vibrational frequency $\omega_{HSi,z}$. For the x and y directions, the vibrational frequencies are $\omega_{HSi,x} = \omega_{HSi,y} = 645$ cm^{-1}. The O-Si value 972 cm^{-1} is the average of the observed values lying between 965-980 cm^{-1} (ref. 30 and 31). [c]Ref. 25 for O-H; ref. 22 for H-Si; ref. 28 for O-Si. [d]The range parameters that enter in the Morse form of the LEPS function; $a_i = (D_i/2\mu_i)^{1/2}(1/\omega_i)$.

of θ, ϕ, and Φ. Thus, each trajectory is generated with the set $(E, b, E_{HSi,0} \theta_0, \phi_0, \Phi_0, \{\xi\}_0)$, where $\{\xi\}_0$ represents the initial values of $\{\xi\} = (\xi_0, \xi_1, ..., \xi_N)$. We sample 30000 sets for each ensemble. We follow each trajectory for 50 ps, which is a sufficiently long time for OH(g) to recede from the influence of surface interaction, to confirm the occurrence of a reactive event forming OH. Furthermore, we confirm that each trajectory can be successfully back-integrated in the computational procedure. We take the chain length of $N = 10$.[14] All pertinent interaction and spectroscopic constants[12,25-31] used in the calculation are listed in Table 1.

Results and Discussion

The main topics to be considered in the present study are the probabilities of OH formation and amounts of energy deposited in the vibrational motion of the product molecule OH varying the initial excitation of the adatom-surface vibration. The results presented are at $T_g = 1500$ K and $T_s = 300$ K. Even though the fraction of H-Si in the ground state is f ($v_{HSi} = 0$) = 1 −
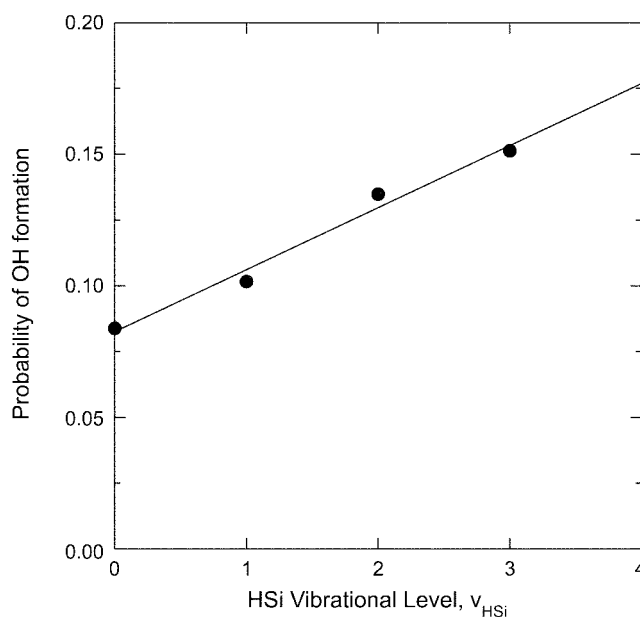

Figure 3. The probabilities of OH formation as a function of the adatom-surface vibrational state.

$e^{-\hbar\omega_{HSi}/kT}$ = 0.9999 at this surface temperature, we have calculated the probabilities of OH formation and amounts of energy deposited in the product molecule OH with the fixed initial excitation of the $v_{HSi} = 0$, 1, 2, and 3, respectively. Nearly all reactive events of 30 000 trajectories sampled occur on the time scale less than 0.3 ps.

A. Reaction Probabilities. As shown in Figure 3, the reaction probability of the OH formation, O(g) + H(ad)/Si → OH(g) + Si, increases linearly with increasing initial excitation of the H-Si vibration. For example, the reaction probability of the OH formation for the H-Si vibration in the ground state is 0.0838. But, when the initial H-Si vibrational

energy level is raised to 3, the probability of OH formation increases to 0.151. The total reaction cross section calculated using the impact parameter-dependent probability function $P(b)$, the opacity function, in the expression $\sigma = 2\pi \int_0^{b_{max}} P(b)\,b\,db$ is 1.78 Å^2 for the OH formation reaction when $v_{HSi} = 0$. It rises to 3.49 Å^2 when v_{HSi} is increased to 3.

The results of the present calculation can be compared with other studies on related gas-surface reactions.[11] The variation of the probability of OH formation with increasing initial excitation of the adatom-surface vibration in the present study is similar to the calculated results of the ER-type hydrogen recombination on a silicon surface. Furthermore, the magnitude of the OH formation probability is not greatly different for the reaction H(g) + H(ad)/Si → H$_2$(g) + Si.[11] We note that in the H$_2$ reaction the adatom-surface bond is the same as that in the present study and the H-to-H interaction energy $D_0^0 = 4.478$ eV[25] is very close to $D_0^0 = 4.392$ eV of the O-to-H interaction in the present study, although the incident atom energy is much lower. In the H$_2$ system, the incident atom energy is 0.030 eV, but we have used the Maxwellian sampling at $T_g = 1500$ K at which the average translational energy is 0.236 eV. Since the reaction exothermicity is largely determined by the bond energies given above, the two reaction systems are energetically similar. Another comparison which can be made is the dependence of the probability of OH formation on the initial state of the HSi vibration. For O(g) + H(ad)/Si, the ratio of the OH formation probability for $v_{HSi} = 1$ to 0 calculated in the present study is 0.102/0.0838 = 1.22. In the related system H(g) + H(ad)/Si → H$_2$(g) + Si at the surface temperature 300 K, which is the same as in the present case, but at E = 0.030 eV, the corresponding ratio is known to be 0.182/0.109 = 1.67.[11] Although they are different reaction, the effect of the initial vibrational excitation on the gas-surface reaction is qualitatively similar.

In Figure 4 we show the dependence of the opacity function $P(b)$ on the impact parameter for the OH formation. We consider the ground state and $v_{HSi} = 3$ state for comparison. This b-dependence provides useful information about the region where the OH formation occurs. For the adatom-surface vibration initially in the ground state, the OH formation occurs in small b collisions ($0 < b < 1.5$ Å), where its $P(b)$ rises rapidly from a small value at $b = 0$ to the maximum value of 0.546 at $b = 0.63$ Å [see Figure 4(a)]. Since the adatom is tilted, the $b = 0$ collision in a three-dimensional reaction does not represent the collinear configuration of O···H-Si. Therefore, the $b = 0$ configuration is not efficient for the flow of energy between the loosely bound O···H bond to the H-Si bond in the short-lived O···H-Si collision complex. The narrowness of the impact parameter range indicates that the OH formation is localized in the neighborhood of the adatom site. Because the HSi bond is tilted, the incident atom hitting H(ad) head-on at $\theta_{inc} = 0$ is 1.514 Å × sin20.6° = 0.533 Å away from the axis normal to the zeroth Si atom. Thus, for example, if we assume the O-to-H distance to be 0.97 Å, the normal OH bond distance, the three atoms (O, H, Si) in the OH formation reaction can align almost collinearly in the $\Phi = 0$ direction when the incident atom reaches the distance with $b \approx 0.34$ Å. In the ± 10% range of the normal OH bond distance, the collinear configuration occurs when the impact parameter lies in the range of 0.31 Å to 0.38 Å. When $v_{HSi} = 3$, Figure 4(b) shows that the probability maximum with a broad peak appears near $b = 1.5$ Å.

A clearer picture of the spatial distribution of OH formation on the surface can be seen by examining the dependence of the reactive events on the azimuthal angle Φ. Such dependence presented in Figure 5 for the HSi vibration initially in the ground state shows a greater propensity of the OH formation in the vicinity of $\Phi = 90°$ and 270°, where the 1st and 5th Si atoms are located, respectively. However, the openness is less along the 3rd Si than along the 1st and 5th sites, so the probability of the OH formation along the $\Phi = 180°$ direction is significantly reduced. The tilting of the adatom in the $\Phi = 0$ direction tends to expose the five surface atoms of the
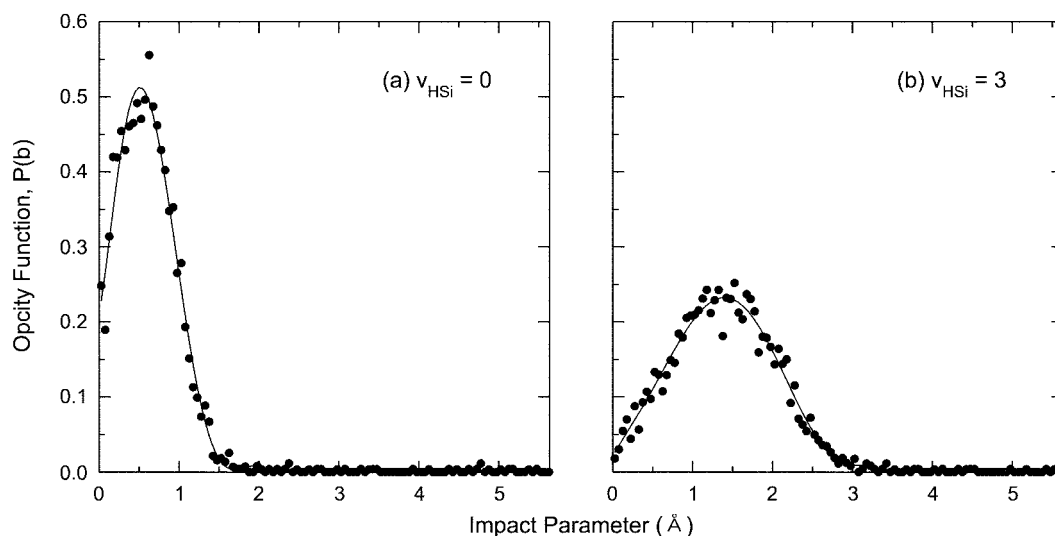

Figure 4. Dependence of the OH formation on the impact parameter for the H-Si vibration initially in $v_{HSi} = 0$ and 3.
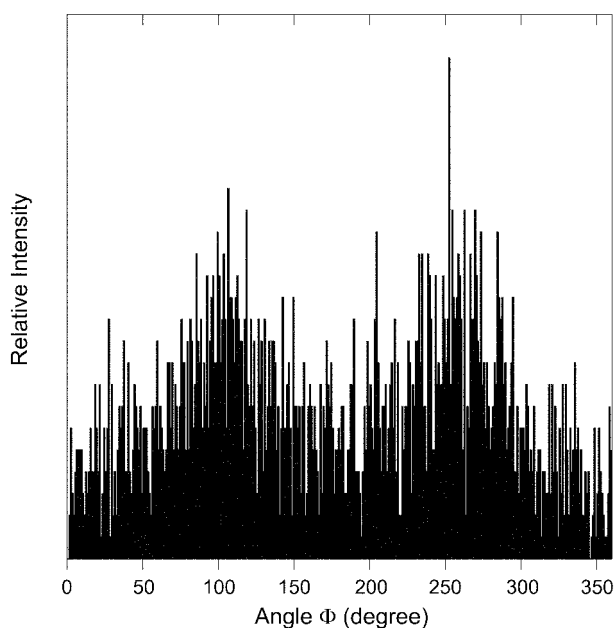
Figure 5. Distribution of the azimuthal angle of the incident angle for the OH formation.

second and third quadrants to the incident gas atom. In this state, the gas atom is loosely bound to the adatom, forming a short-lived complex O⋯H-Si. Since the Si-Si dimer distance is 2.52 Å (*e.g.*, between the zeroth and the 3rd Si) and the Si-Si distance along the dimer strand is 3.87,[22] we expect the openness of this region to steer efficiently the gas atom to stay bound at the adatom site, thus enhancing the reactive event O(g) + H(ad)/Si → OH(g) + Si. Since the adatom and the 3rd Si site compete for the incident atom approaching the region between these two atoms (*i.e.*, $\Phi \approx 180°$), the probability of OH formation is smaller in this region (see Figure 5). In Figures 6(a) and 6(b), we compare the $\Phi = 90°$ and 180° PES, for the reaction taking place at $b = 0.5$ Å. Here we set $\theta = \phi = 0°$,

so the 90° and 270° surfaces are equivalent. The openness of the 90° surface is clearly seen. The barrier occurs at −3.655 eV, which is lower than the entrance channel at −3.645 eV by 0.010 eV. Furthermore, the potential well in the entrance channel is 0.010 eV below the barrier. Thus, the channel is wide open for the incident atom. On the other hand, in the $\Phi = 180°$ direction, where the adatom and the 3rd Si atom compete for the oxygen atom, the barrier is 0.090 eV higher than the entrance channel. Thus, the energy surface is much less open compared with the 90° case, especially for the low energy incident atom, and the probability of OH formation is less than in the 90° case.

Along the $\Phi = 0$ direction, the distance between the nearest Si atoms belonging to the two adjacent strands is as large as 5.15 Å, so there is no effective steering of the incident atom approaching the surface with a smaller impact parameter by the 7th Si for the OH formation. Thus, we find the appearance of a regiospecificity for OH formation around the adatom and above the surface from this Φ dependence.

B. Product Energy Distribution. The energy available for OH and the surface after the adatom-surface bond dissociation is $(\Delta D_0^0 + E_{HSi}^0 + E)$ eV, where E_{HSi}^0 is the initial energy of the adatom-surface vibration and E is the oxygen atom kinetic energy. The reaction exothermicity ΔD_0^0 is the difference between the H-Si dissociation energy and the OH dissociation energy. From the dissociation energies listed in Table 1, we find $\Delta D_0^0 = 0.892$ eV for this exothermic reaction, which is characterized by an attractive PES shown in Figure 2. In Table 2, we summarize the distribution of the ensemble-averaged energies deposited in OH as well as that propagated into the solid for $v_{HSi} = 0, 1, 2$ and 3. The calculation of the energy deposited in OH from the computer output is straightforward. The translational energy is $E_{trans,OH} = \frac{1}{2}m_{OH}(\dot{Z} - \gamma_H \cos\theta_{inc} r_{OH})^2$, where $m_{OH} = (m_O + m_H)$ and $\gamma_H = m_H/(m_O + m_H)$. The rotational energy is $E_{rot,OH} = L_{OH}^2/2\mu_{OH}r_{OH}^2$, where the angular momentum $L_{OH} = \mu_{OH}(z\dot{\rho} - \rho\dot{z})$ with the

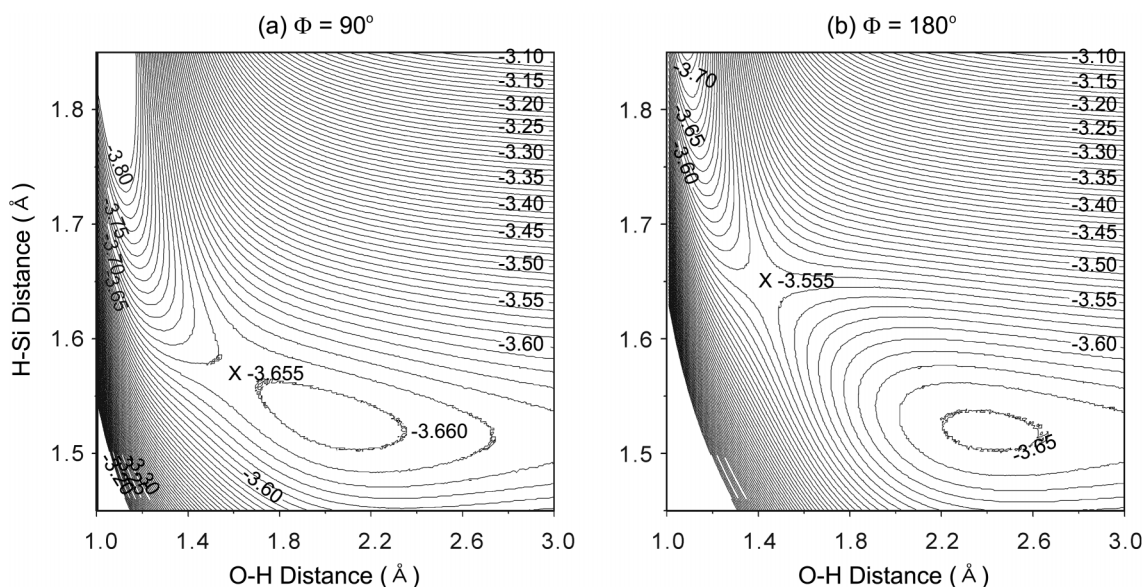**Figure 6**. Potential energy surfaces for (a) $\Phi = 90°$ and (b) $\Phi = 180°$ at $b = 0.50$ Å.

corresponding quantum number $J_{OH} = L_{OH}/\hbar$. The equation for the OH vibrational energy takes the usual expression $E_{vib,OH} = \frac{1}{2}\mu_{OH}\dot{r}_{OH}^2 + D_{OH}[1 - e^{(r_{OH,e} - r_{OH})/2a}]^2$, where a is the range parameter and $r_{OH,e}$ is the equilibrium value of r_{OH}. The expression for the energy propagated from the reaction zone into the solid through the $(N+1)$-atom chain is[14]

$$E_{s,OH} = \frac{1}{2}M_s \sum_{i=0}^{N} \dot{\xi}_i^2(t) + \frac{1}{2}M_s \sum_{i=0}^{N-1} \omega_{e,i}^2 \xi_i^2(t) + \frac{1}{2}M_s\Omega_N^2\xi_N^2(t)$$

$$+ M_s \sum_{i=0}^{N-1} \omega_{c,i+1}^2 \xi_i(t)\xi_{i+1}(t).$$

We average all these energies over the ensemble of reactive trajectories to obtain the quantities $<E_{trans,OH}>$, $<E_{rot,OH}>$, $<E_{vib,OH}>$ and $<E_{s,OH}>$. For $v_{HSi} = 0$, the energies deposited in the translational, rotational and vibrational motions of OH are $<E_{trans,OH}>$ = 0.398 eV, $<E_{rot,OH}>$ = 0.199 eV, and $<E_{vib,OH}>$ = 0.389 eV. The amount of energy propagated into the solid $<E_{s,OH}>$ is only 0.053 eV. Thus, the gas-phase product OH carries away about 95% of the energy released in the reaction. We find that 76% of the available energy deposits in the translational and vibrational motions, thus resulting in substantial kinetic and internal (vibrational) excitation with only a small portion of the available energy lost to the surface. This type of product energy distribution with a major portion depositing in translation and vibration is characteristic of an ER mechanism.[13,32] Increasing the initial vibrational state of the adatom-surface vibration from $v_{HSi} = 0$ to 1, 2, and 3 causes a large increase in the OH vibrational energy, while the energies of all other motions

Table 2. Distribution of the reaction exothermicity for O(g) + H(ad)/Si. The ensemble-averaged energies are in eV

v_{HSi}	$<E_{trans,OH}>$	$<E_{rot,OH}>$	$<E_{vib,OH}>$	$<E_{s,OH}>$
0	0.398 (38.3)[a]	0.199 (19.2)	0.389 (37.4)	0.053 (5.10)
1	0.388 (31.6)	0.185 (15.1)	0.598 (48.7)	0.056 (4.56)
2	0.387 (27.6)	0.184 (13.1)	0.773 (55.0)	0.060 (4.27)
3	0.377 (22.9)	0.207 (12.6)	1.000 (60.7)	0.063 (3.82)

[a]The numbers in the parentheses are the % fraction of the total energy released in the reaction.

change by only a few percent.

C. Vibrational Energy of the Product Molecules. As shown in Table 2, the ensemble-averaged vibrational energy increases linearly with increasing v_{HSi}, while the amounts of energy deposited in all other motions vary only slightly. When $v_{HSi} = 1$, the amount of energy deposited in the vibrational motion increases by 0.209 eV to 0.598 eV from the $v_{HSi} = 0$ value, a 54% increase. This increase corresponds to the OH vibration taking more than 80% of the H-Si vibrational energy above the HSi ground state. The variation of the OH vibrational energy with the initial state of the H-Si vibration indicates the preferential flow of vibrational energy from the HSi bond to the vibration of the newly formed OH. This efficient energy flow occurs at close range of the O(g) and H(ad)/Si interaction. In this range, the incident oxygen atom is loosely bound to the surface, forming a short-lived collision complex (O···H-Si), where the two bond modes are coupled during the asymmetric stretch. The frequency of the vibrational motion of O···H starts with a low value and increases toward the final OH value of 3738 cm^{-1}. When this frequency changes as the OH bond tends to stabilize, it passes through the vibrational frequency of the H-Si bond, 2093 cm^{-1}, near and at which frequency "intra-molecular" HSi vibration to OH vibration energy transfer (VV) takes place efficiently. Such near-resonant or resonant energy transfer is known to be the principal energy pathway in molecular collisions, ranging from diatomic to polyatomic molecules.[33,34]

In Figure 7, we show the vibrational population. Here the distribution is determined by assigning the quantum number v_{OH} determined as $v_{OH} = \text{int}[E_{vib,OH}/E_{vib}(v_{OH})]$, the integer nearest to the ratio $E_{vib,OH}/E_{vib}(v_{OH})$. Here $E_{vib}(v_{OH})$ is the vibrational energy determined from the eigenvalue expression $E_{vib}(v_{OH})/hc = \omega_e(v_{OH}) - \omega_e x_e(v_{OH} + \frac{1}{2})^2$ with $\omega_e = 3737.76$ cm^{-1} and $\omega_e x_e = 84.881$ cm^{-1}.[26] For $v_{HSi} = 0$, the intensity of vibrational population for $v_{OH} = 1$ is 0.376 compared with 0.610 for $v_{OH} = 0$ (or the $v_{OH} = 1$ to $v_{OH} = 0$ population ratio 0.616). The $v_{OH} = 1$ population is significantly larger than that predicted by the Boltzmann distribution, thus representing the occurrence of a substantial vibrational excitation. Even at 1500 K, the Boltzmann distribution gives the fractions $f(v_{OH}$
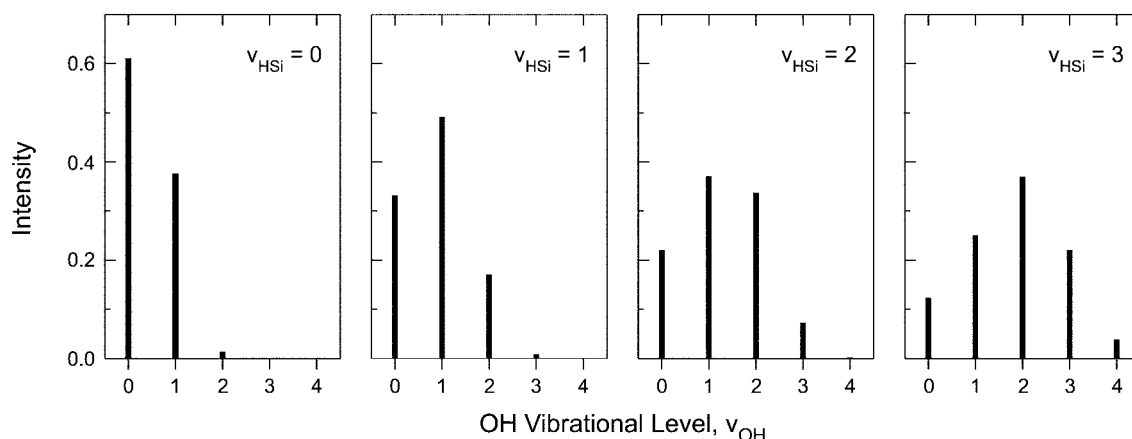

Figure 7. Vibrational population distribution of OH.

$= 0) = 1 - e^{-\hbar\omega/kT} = 0.972$ and $f(v_{OH} = 1) = [1 - e^{-\hbar\omega/kT} = 0.027$, *i.e.*, $f(v_{OH} = 1)/f(v_{OH} = 0)$ is only 0.028, so the vibrational population distribution of OH produced on the silicon surface seriously deviates from the prediction of the Boltzmann distribution law. The deviation becomes very serious when v_{HSi} is raised. For example, for $v_{HSi} = 1$, the population intensity of $v_{OH} = 1$ is now greater than that of $v_{OH} = 0$, a population inversion.[35] As shown in Figure 7, the inversion becomes stronger as we raise the initial excitation to the v_{HSi} = 2 and 3 states. For example, for $v_{HSi} = 3$, the $v_{OH} = 2$ to v_{OH} = 0 population ratio is as large as 3.01. For this initial excitation, we find the formation of OH even in an excited state as high as $v_{OH} = 5$, although the population intensity is only 0.0144 (not shown in Figure 7).

Concluding Comments

Trajectory calculations of the O(g) + H(ad)/Si reaction using the MTGLE approach show a moderate extent of the OH formation at gas temperature 1500 K and surface temperature 300 K. A major portion of the available energy for the reaction deposits in the translational and vibrational motions of the newly formed OH(g), resulting in substantial kinetic and vibrational excitations. The product molecule is ejected from the surface on a subpicosecond time scale in a small impact parameter collision before thermal equilibration can occur.

The energy initially stored in the adatom-surface vibrational motion preferentially deposits in the vibrational motion of OH, representing an efficient intramolecular vibration-to-vibration energy flow in the short-lived collision complex. The vibrational population of OH does not follow the Boltzmann distribution and depends strongly on the initial state of the adatom-surface vibration. Except for the H-Si vibration initially in the ground state, OH formed in the reaction with all other initial excitation exhibits a vibrational population inversion.

The amount of energy propagated into the solid is one-twentyth the available energy, and this energy varies only slightly with increase of the vibrational state of the adatom-surface bond.

References

1. Shustorovich, E. *Surf. Sci. Rep.* **1986**, *6*, 1.
2. Christmann, K. *Surf. Sci. Rep.* **1988**, *9*, 1.
3. Weast, R. C., Ed.; *CRC Handbook of Chemistry and Physics*, 64th Ed.; CRC Press: 1983; pp F176-F181.
4. Hall, R. I.; Cadez, I.; Landau, M.; Pichou, F.; Schermann, C. *Phys. Rev. Lett.* **1988**, *60*, 337.
5. Eenshuistra, P. J.; Bonnie, J. H. M.; Lois, J.; Hopman, H. *Phys. Rev. Lett.* **1988**, *60*, 341.
6. Kratzer, P.; Brenig, W. *Surf. Sci.* **1991**, *254*, 275.
7. Jackson, B.; Persson, M. *Surf. Sci.* **1992**, *269*, 195.
8. Schermann, C.; Pichou, F.; Landau, M.; Cadez, I.; Hall, R. I. *J. Chem. Phys.* **1994**, *101*, 8152.
9. Weinberg, W. H. In *Dynamics of Gas-Surface Interactions*; Rettner, C. T.; Ashfold, M. N. R., Eds.; Royal Society of Chemistry: 1991; pp 171-219.
10. Shin, H. K. *J. Phys. Chem. A* **1998**, *102*, 2372.
11. Koleske, D. D.; Gates, S. M.; Jackson, B. *J. Chem. Phys.* **1994**, *101*, 3301.
12. Kratzer, P. *J. Chem. Phys.* **1997**, *106*, 6752.
13. Buntin, S. A. *J. Chem. Phys.* **1998**, *108*, 1601.
14. Kim, Y. H.; Ree, J.; Shin, H. K. *J. Chem. Phys.* **1998**, *108*, 9821.
15. Kim, Y. H.; Ree, J.; Shin, H. K. *Chem. Phys. Lett.* **1999**, *314*, 1.
16. Ree, J.; Chang, K. S.; Moon, K. H.; Kim, Y. H. *Bull. Korean Chem. Soc.* **2001**, *22*, 889.
17. Ree, J.; Kim, Y. H.; Shin, H. K. *Chem. Phys. Lett.* **2002**, *353*, 368.
18. Ko, Y.; Ree, J.; Kim, Y. H.; Shin, H. K. *Bull. Korean Chem. Soc.* **2002**, *23*, 1737.
19. Ree, J.; Shin, H. K. *J. Chem. Phys.* **1999**, *111*, 10261.
20. Adelman, S. A. *Adv. Chem. Phys.* **1980**, *44*, 143.
21. McDowell, H. K. *J. Chem. Phys.* **2000**, *112*, 6971.
22. Radeke, M. R.; Carter, E. A. *Phys. Rev. B* **1996**, *54*, 11803.
23. *American Institute of Physics Handbook*, 3rd Ed.; Gray, D. E., Ed.; McGraw-Hill: 1972; pp 4-116.
24. Ree, J.; Kim, Y. H.; Shin, H. K. *J. Chem. Phys.* **1996**, *104*, 742.
25. Huber, K. P.; Herzberg, G. *Constants of Diatomic Molecules*; Van Nostrand Reinhold: 1979.
26. Van de Walle, C. G.; Street, R. A. *Phys. Rev. B* **1995**, *51*, 10615.
27. Kratzer, P.; Hammer, B.; Norskov, J. K. *Phys. Rev. B* **1995**, *51*, 13432.
28. Jenichen, A.; Johansen, H. *Surf. Sci.* **1988**, *203*, 143.
29. Tully, J. C.; Chabal, Y. J.; Raghavachari, K.; Bowman, J. M.; Lucchese, R. R. *Phys. Rev. B* **1985**, *31*, 1184.
30. Huffman, M.; McMillan, P. *J. Non-Cryst. Solids* **1985**, *76*, 369.
31. Krol, J. M.; Rabinovich, E. M. *J. Non-Cryst. Solids* **1986**, *82*, 143.
32. Gross, A. *Surf. Sci. Rep.* **1998**, *32*, 291.
33. Yardley, J. T. *Introduction to Molecular Energy Transfer*; Academic: 1980; Chapter 5.
34. Shin, H. K. *J. Phys. Chem. A* **2000**, *104*, 6699.
35. Kori, M.; Halpern, B. L. *Chem. Phys. Lett.* **1984**, *110*, 223.